ACS OMEGA

Article

Cite This: ACS Omega 2017, 2, 7281-7292

http://pubs.acs.org/journal/acsodf

Efficient Synthesis of Amine-Linked 2,4,6-Trisubstituted Pyrimidines as a New Class of Bacterial FtsZ Inhibitors

Kin-Fai Chan,*[,†] Ning Sun,[†] Siu-Cheong Yan,[†] Iris L. K. Wong,[†] Hok-Kiu Lui,[†] Kwan-Choi Cheung,[†] Jian Yuan,[†] Fung-Yi Chan,[†] Zhiwei Zheng,[§] Edward W. C. Chan,[†] Sheng Chen,[†,§] Yun-Chung Leung,[†] Tak Hang Chan,[†,‡] and Kwok-Yin Wong*[,†]

[†]State Key Laboratory of Chirosciences and Department of Applied Biology and Chemical Technology, The Hong Kong Polytechnic University, Hung Hom, Kowloon, Hong Kong SAR, China

[‡]Department of Chemistry, McGill University, Montreal, Quebec H3A 2K6, Canada

[§]Shenzhen Key Laboratory for Food Biological Safety Control, Food Safety and Technology Research Centre, The Hong Kong PolyU Shenzhen Research Institute, Shenzhen 518057, China

Supporting Information

ABSTRACT: We have recently identified a new class of filamenting temperature-sensitive mutant Z (FtsZ)-interacting compounds that possess a 2,4,6-trisubstituted pyrimidine−quinuclidine scaffold with moderate antibacterial activity. Employing this scaffold as a molecular template, a compound library of amine-linked 2,4,6-trisubstituted pyrimidines with 99 candidates was successfully established by employing an efficient convergent synthesis designed to explore their structure−activity relationship. The results of minimum inhibitory concentration (MIC) assay against *Staphylococcus aureus* strains and cytotoxicity assay against the mouse L929 cell line identified those compounds with potent antistaphylococcal properties (MIC ranges from 3 to 8 μg/mL) and some extent of cytotoxicity against normal cells (IC_{50} ranges from 6 to 27 μM). Importantly, three compounds also exhibited potent antibacterial activities against nine clinically isolated methicillin-resistant *S. aureus* (MRSA) strains. One of the compounds, **14av_amine16**, exhibited low spontaneous frequency of resistance, low toxicity against *Galleria mellonella* larvae, and the ability to rescue *G. mellonella* larvae (20% survival rate at a dosage of 100 mg/kg) infected with a lethal dose of MRSA ATCC 43300 strain. Biological characterization of compound **14av_amine16** by saturation transfer difference NMR, light scattering assay, and guanosine triphosphatase hydrolysis assay with purified *S. aureus* FtsZ protein verified that it interacted with the FtsZ protein. Such a property of FtsZ inhibitors was further confirmed by observing iconic filamentous cell phenotype and mislocalization of the Z-ring formation of *Bacillus subtilis*. Taken together, these 2,4,6-trisubstituted pyrimidine derivatives represent a novel scaffold of *S. aureus* FtsZ inhibitors.

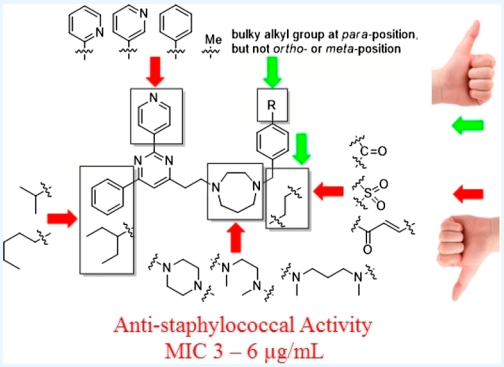

1. INTRODUCTION

The inexorable rise in the incidence of serious bacterial infections caused by multiple antibiotic-resistant bacteria in health care- and community-associated settings has become a pressing threat of public health worldwide.[1] Of particular concern is the rise in the incidence of methicillin-resistant *Staphylococcus aureus* (MRSA) infections. MRSA can cause a wide range of illnesses, from mild skin and wound infections to pneumonia and bloodstream infections that cause sepsis and death. The Centers for Disease Control and Prevention of the United States estimates that over 80 000 severe MRSA infections occur annually, resulting in 11 000 deaths.[2] This scenario has driven the search for novel classes of antistaphylococcal agents which act on novel bacterial drug targets.

The bacterial cell division machinery has been considered as an important field for exploring potential novel drug targets of antibacterial agents.[3] The filamenting temperature-sensitive mutant Z (FtsZ) protein undoubtedly represents one of the well-characterized and exploitable antibacterial drug targets.[4−10] FtsZ is a cytoplasmic protein and highly conserved tubulin-like guanosine triphosphatase (GTPase), playing an important role in bacterial cell division. In order for bacteria to carry out cell division, FtsZ monomers are required to localize mid cells through the precise positioning of cell division site positioning proteins and self-polymerize into single stranded straight protofilaments by means of head-to-tail association that curve upon the hydrolysis of guanosine triphosphate (GTP) molecules.[11] Consecutive lateral contacts between FtsZ protofilaments produce FtsZ bundles, which eventually lead

Received: May 30, 2017
Accepted: September 12, 2017
Published: October 27, 2017

DOI: 10.1021/acsomega.7b00701
ACS Omega 2017, 2, 7281−7292

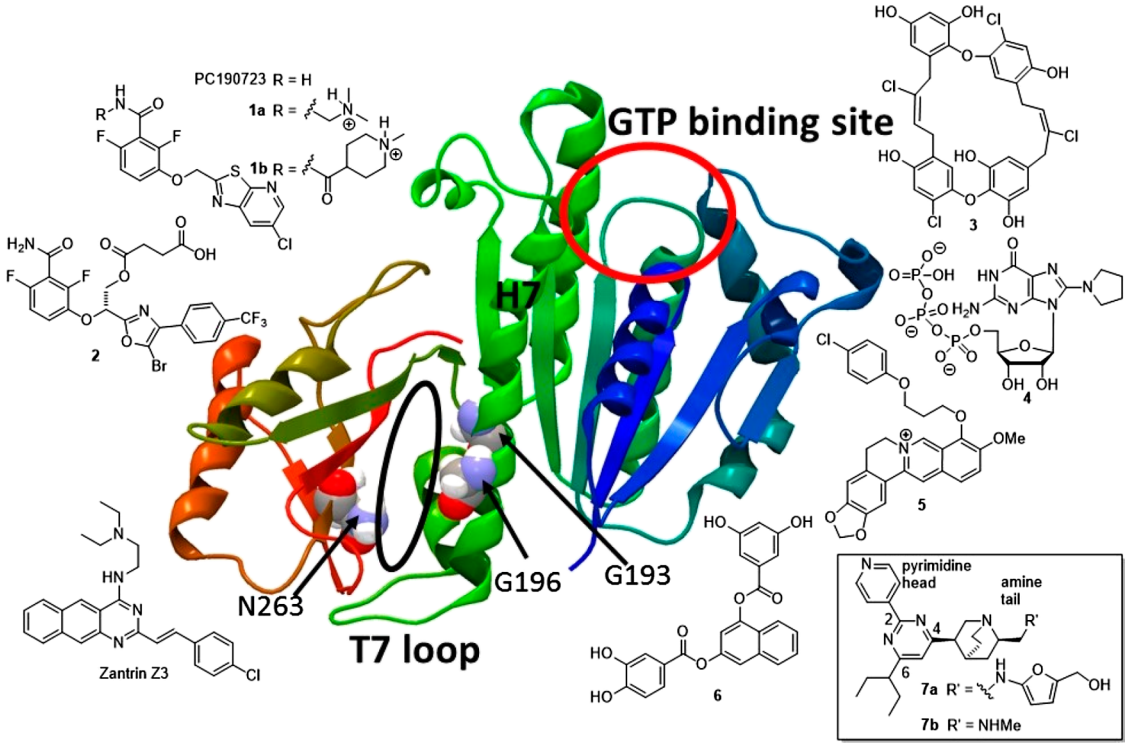

Figure 1. Crystal structure of *S. aureus* FtsZ (PDB ID: 4DXD) with labeled GTP-binding site (red circle), T7 loop, central H7, and amino acids at positions 193, 196, and 263. The black oval indicates the binding site of PC190723. The chemical structures of PC190723, zantrin Z3, and FtsZ inhibitors **1**−**7** are shown.

to the formation of a contractile ring called Z-ring at the mid cell. Following the subsequent involvement of other downstream cell division proteins, Z-ring contraction and depolymerization complete the cell division process to furnish identical daughter cells. Small molecules interfering the initial stage of the FtsZ polymerization are capable of blocking bacterial cell division, causing the abrogation of bacterial cell viability eventually. These types of compounds have great potential to be developed as efficacious antimicrobial agents with a novel mode of action for clinical applications. Several high-resolution X-ray crystal structures of FtsZ homologues have been reported.[12] These results contributed to the knowledge regarding the general organization of the FtsZ protein structure, which is known to comprise two independent folding domains (Figure 1). The N-terminal domain forms a nucleotide-binding site (GTP-binding site, the upper red circle of Figure 1), whereas the C-terminal domain contains a flexible loop (T7 loop). Both the domains were interconnected via a long central helix 7 (H7) of high rigidity.

Many FtsZ-interacting compounds have been discovered and reported to bind either the GTP-binding site or a cleft formed by the H7, T7 loop, and C-terminal β sheet (Figure 1, black oval). Some exhibit potent antibacterial activity with minimum inhibitory concentration (MIC) at the micromolar range. PC190723 (Figure 1, top left)[13−15] and its prodrugs **1a**,[16] **1b**,[17−19] and benzamide **2**[20] have been demonstrated to exhibit in vitro and in vivo efficacy in a murine infection model. Moreover, X-ray crystallographic analysis revealed that PC190723 binds to a narrow cleft formed by the H7, T7 loop, and C-terminal β sheet (Figure 1, black oval).[21] However, analysis of PC190723 drug-resistant mutants across various MRSA strains revealed that all PC190723 drug-resistant isolates had multiple mutations, resulting in amino acid substitutions that mapped to the FtsZ protein.[22] These mutations mainly occurred at amino acid positions 193, 196, and 263 (Figure 1), which accounted for over 90% of PC190723 drug-resistant mutants. These results suggested that amino acid substitutions can alter slightly the overall shape of the binding pocket without interfering the normal function of FtsZ. Nevertheless, this change resulted in PC190723 no longer binding to this pocket, therefore causing drug resistance. Such findings may hinder the potential of PC190723 and other related compounds[23] from being developed into agents that exhibit the potential to target the same binding pocket for further clinical development. On the other hand, several compounds targeting the GTP-binding site of FtsZ have also been demonstrated to exhibit potent antibacterial activity, including zantrin Z3,[24,25] natural product chrysophaentin A **3**,[26] C8-substituted GTP analogues **4**,[27,28] berberine analogues **5**,[29,30] and naphthol derivatives **6**[31,32] (Figure 1, right). Surprisingly, among these inhibitors, no drug-resistant mutants have been reported in the literature so far, presumably because of the fact that the GTP-binding site is very important for recognizing the GTP molecules. Amino acid substitutions at this binding pocket may cause improper recognition of GTP molecules and thus hinder normal GTP hydrolysis process, therefore losing the energy source to drive the polymerization of FtsZ monomers. We reasoned that specially designed small molecules, which can mimic and compete with GTP molecules to bind the GTP-binding site of FtsZ, may have greater potential to be developed as antimicrobial agents without acquiring drug resistance.

To take advantage of this idea, we have employed a combined approach of high-throughput virtual screening and biological evaluation of natural product libraries to discover compounds with new chemical scaffolds that target the GTP-

DOI: 10.1021/acsomega.7b00701
ACS Omega 2017, 2, 7281−7292

Scheme 1[a]

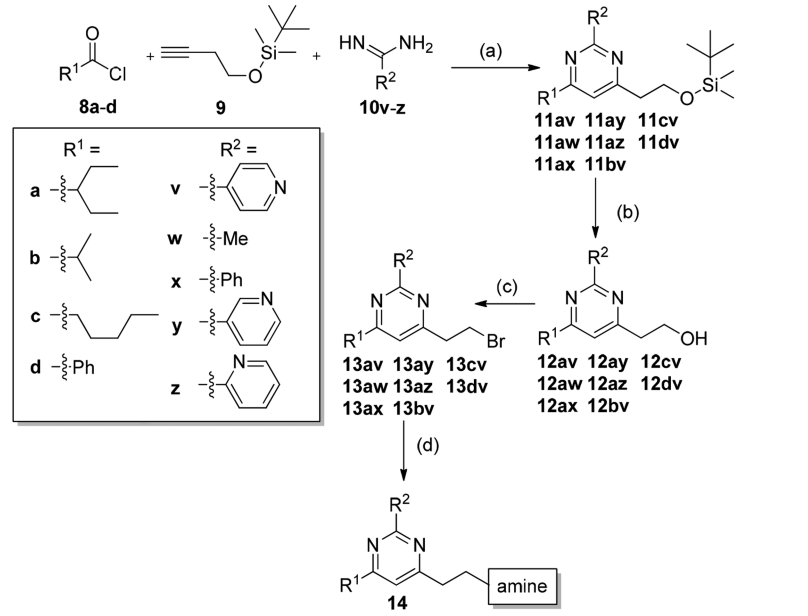

14av_amine01	14av_amine23	14ax_amine06	14bv_amine02	14dv_amine02
14av_amine02	14av_amine24	14ax_amine07	14bv_amine04	14dv_amine06
14av_amine03	14av_amine25	14ax_amine16	14bv_amine05	14dv_amine07
14av_amine04	14av_amine26	14ay_amine04	14bv_amine08	14dv_amine08
14av_amine05	14av_amine27	14ay_amine05	14bv_amine10	14dv_amine09
14av_amine06	14av_amine28	14ay_amine08	14bv_amine11	14dv_amine10
14av_amine07	14av_amine29	14ay_amine09	14bv_amine12	14dv_amine12
14av_amine08	14av_amine30	14ay_amine12	14bv_amine13	14dv_amine16
14av_amine09	14av_amine31	14ay_amine13	14bv_amine14	14dv_amine20
14av_amine10	14av_amine32	14ay_amine16	14bv_amine15	
14av_amine11	14av_amine33	14ay_amine17	14bv_amine16	
14av_amine12	14av_amine34	14ay_amine18	14bv_amine17	
14av_amine13	14av_amine35	14ay_amine20	14bv_amine18	
14av_amine14	14av_amine36	14az_amine07	14cv_amine02	
14av_amine15	14av_amine37	14az_amine08	14cv_amine06	
14av_amine16	14av_amine38	14az_amine09	14cv_amine09	
14av_amine17	14av_amine39	14az_amine12	14cv_amine16	
14av_amine18	14aw_amine06	14az_amine16		
14av_amine19	14aw_amine07	14az_amine17		
14av_amine20	14aw_amine16	14az_amine18		
14av_amine21		14az_amine20		
14av_amine22				

[a](a) (i) 2 mol % $Pd(PPh_3)_2Cl_2$, 4 mol % CuI, NEt_3, tetrahydrofuran (THF), rt 1−2 h and (ii) Na_2CO_3, reflux 14 h; (b) concn HCl, MeOH, rt 2 h; (c) PPh_3, CBr_4, THF, rt 3−4 h; and (d) **amine01−39** (refer to Chart 1 for chemical structures), ACN, rt 24 h.

binding site of the FtsZ protein. Our previous study identified a new class of FtsZ inhibitor **7** bearing a 2,4,6-trisubstituted pyrimidine and a chiral aminoquinuclidine moiety (Figure 1, bottom right).[33] This class of compounds has been demonstrated to inhibit the GTPase hydrolysis activity of *S. aureus* FtsZ at a low micromolar IC_{50} value with moderate antimicrobial activity against *S. aureus* and *Escherichia coli*. Compound **7a** also exhibited a strong synergistic effect against various MRSA and vancomycin-resistant *Enterococcus faecium* strains when combined with clinically used *β*-lactam antibiotics.[34] However, the structural complexity of the chiral quinuclidine scaffold and limited compound availability from commercial sources have prevented further development. In the present study, we report a design and efficient synthesis of a novel amine-linked 2,4,6-trisubstituted pyrimidine compound library with the aims of simplifying the complex quinuclidine scaffold with simple amines and improving their antimicrobial activity. A promising compound exhibiting potent antimicrobial activity has been selected for further investigation regarding its interaction with the *S. aureus* FtsZ protein. Because of its structural novelty, potent antimicrobial activity, and high selectivity against *S. aureus*, a new series of such compounds may represent a promising starting point for further investigation.

2. RESULTS AND DISCUSSION

2.1. Compound Library Design and Synthesis.

Molecular docking study of compound **7** and GTP molecules using *S. aureus* FtsZ revealed that the 2,4,6-trisubstituted pyrimidine moiety of **7** occupied exactly the same binding pocket as the guanosine moiety of GTP molecules through an extensive network of hydrogen bonds with the FtsZ protein, suggesting that the pyrimidine moiety is crucial for binding.[33] Therefore, our molecular design strategy is to retain the pyrimidine moiety and replace the chiral quinuclidine moiety at position 4 with various substituted amine moieties, which offer

DOI: 10.1021/acsomega.7b00701
ACS Omega 2017, 2, 7281−7292

Chart 1. Chemical Structures of Amines Used in This Study

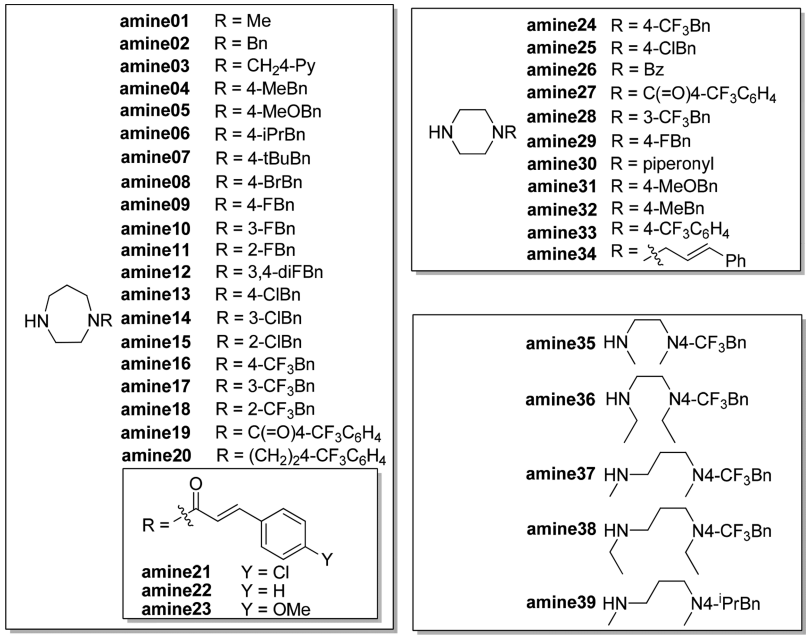

Scheme 2[a]

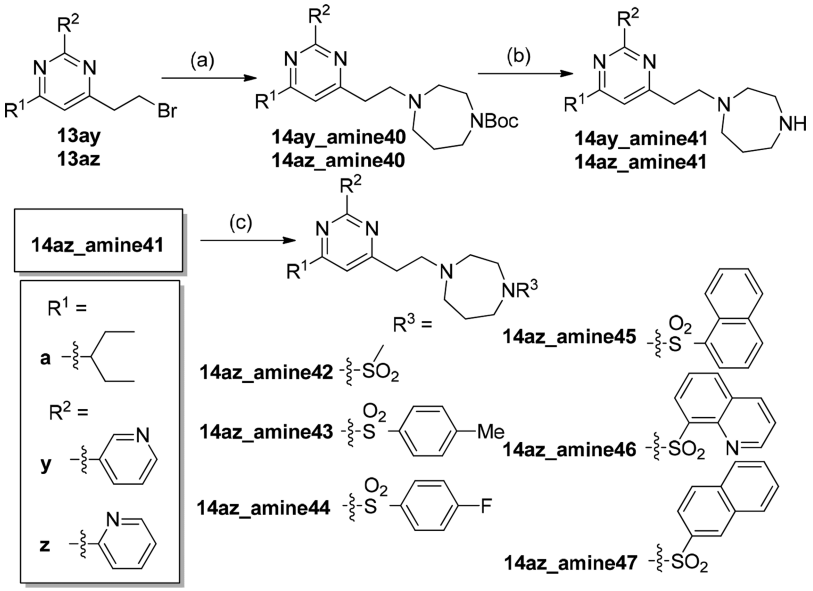

[a](a) 1-Boc-homopiperazine, ACN, rt, 14 h; (b) TFA, DCM, 0 °C, 2 h; and (c) various sulfonyl chlorides, NEt_3, DCM, 0 °C, 3 h.

desirable compound flexibility and physicochemical property.[35] At the same time, various substituents will be installed at positions 2 and 6. As there was no structural information to guide the compound design, compound **7** was therefore divided into two parts (pyrimidine head and amine tail), as outlined in Figure 1. A compound library would then be designed and synthesized to sequentially interrogate the pyrimidine head and the amine tail using convergent synthesis. With the preliminary structure−activity relationship (SAR) in hand, compounds combining the promising structural motifs would then be synthesized by dedicated synthesis. On the basis of this approach, eight pyrimidine heads (Scheme 1) and 39 secondary amine tails (Chart 1) were designed and synthesized. Cyclic amine tails (for a seven-member homopiperazine ring, **amine01−23**, or for a six-member piperazine ring, **amine24−34**) and linear amine tails (**amine35−39**) were included in this study for comparison purpose. A general synthesis route of target compounds **14** is outlined in Scheme 1. The pyrimidine heads were easily obtained by the coupling of various acid chlorides **8a−d** with silyl group-protected terminal alkyne **9** in the presence of triethylamine under Sonogashira conditions, followed by the subsequent addition of excess amidinium hydrochloride salts **10v−z** in one pot, allowing a straightforward access to 2,4,6-trisubstituted pyrimidines **11** under mild conditions and in good yields.[36] It is worthy to note that the use of unprotected terminal alkyne **9** should be avoided because of the relatively low yield of product. Deprotection of the silyl group of **11** by acidic treatment of concentrated hydrochloric

DOI: 10.1021/acsomega.7b00701
ACS Omega 2017, 2, 7281−7292

Table 1. MIC and IC_{50} Values of 2,4,6-Trisubstituted Pyrimidines against *S. aureus* 29213, *E. coli* ATCC 25922, and L929 Murine Fibroblast Cell Lines as Well as Calculated Selectivity Index (SI)[a]

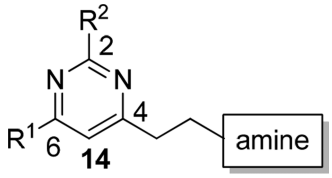

					MIC[#]			
entry	compound no.	R^1	R^2	amine no.	*S. aureus*	*E. coli*	L929 IC_{50}*	SI^
1	**7a**	N.A.	N.A.	N.A.	24 (51)	32	36 ± 2	0.7
2	**7b**	N.A.	N.A.	N.A.	64 (125)	64	N.D.	N.D.
3	**14dv_amine16**	phenyl	4-Py	**16**	3 (5)	>64	7 ± 1	1.4
4	**14dv_amine06**	phenyl	4-Py	**06**	3 (5)	>64	6 ± 1	1.2
5	**14dv_amine20**	phenyl	4-Py	**20**	3 (5)	>64	6 ± 1	1.2
6	**14dv_amine07**	phenyl	4-Py	**07**	3 (5)	>64	6 ± 1	1.2
7	**14dv_amine08**	phenyl	4-Py	**08**	3 (5)	>64	7 ± 1	1.4
8	**14av_amine16**	3-pentyl	4-Py	**16**	4 (8)	>64	8 ± 1	1.0
9	**14av_amine20**	3-pentyl	4-Py	**20**	4 (8)	>64	7 ± 1	0.9
10	**14cv_amine06**	*n*-pentyl	4-Py	**06**	6 (10)	>64	7 ± 2	0.7
11	**14cv_amine16**	*n*-pentyl	4-Py	**16**	6 (10)	>64	9 ± 1	0.9
12	**14dv_amine12**	phenyl	4-Py	**12**	6 (10)	>64	9 ± 1	0.9
13	**14dv_amine10**	phenyl	4-Py	**10**	6 (10)	>64	8 ± 1	0.8
14	**14av_amine28**	3-pentyl	4-Py	**28**	6 (10)	>64	27 ± 1	2.7
15	**14av_amine38**	3-pentyl	4-Py	**38**	6 (10)	>64	14 ± 1	1.4
16	**14av_amine39**	3-pentyl	4-Py	**39**	6 (10)	>64	9 ± 1	0.9
17	**14av_amine24**	3-pentyl	4-Py	**24**	6 (12)	>64	15 ± 2	1.3
18	**14av_amine35**	3-pentyl	4-Py	**35**	6 (12)	>64	10 ± 1	0.8
19	**14av_amine13**	3-pentyl	4-Py	**13**	6 (13)	>64	10 ± 1	0.8
20	**14av_amine06**	3-pentyl	4-Py	**06**	8 (16)	>64	8 ± 2	0.5
21	**14av_amine07**	3-pentyl	4-Py	**07**	8 (16)	>64	9 ± 2	0.6
22	**14av_amine08**	3-pentyl	4-Py	**08**	8 (16)	>64	8 ± 2	0.5
23	**14av_amine17**	3-pentyl	4-Py	**17**	8 (16)	>64	15 ± 1	0.9
24	**14av_amine18**	3-pentyl	4-Py	**18**	8 (16)	>64	18 ± 2	1.1

[a]N.A.: not applicable; N.D.: not determined; [#] MIC, μg/mL; for *S. aureus*, the number in the parentheses is the MIC value calculated in the unit of μM; * concentration of a compound that is required for 50% inhibition (IC_{50}), μM, $N = 1-3$ independent experiments, and the values are presented as mean ± standard error of mean; and ^ SI, it was calculated using the formula L929 IC_{50} (μM)/MIC value of *S. aureus* (μM).

acid in methanol afforded alcohols **12** in quantitative yield, which were further treated with triphenylphosphine and carbon tetrabromide to furnish the bromides **13** in high yield (two steps). It is also worthy to note that bromides **13** were found to be unstable at high temperatures (>50 °C) or under prolonged exposure of weakly basic medium at room temperature, affording the elimination product of 4-vinyl pyrimidine. It is recommended that bromides **13** should be prepared freshly and used immediately for the next step. The compound library of amine-linked 2,4,6-trisubstituted pyrimidines **14** was then constructed by mixing the freshly prepared bromides **13** with various amine derivatives **amine01−39** (Chart 1) in acetonitrile (ACN) at room temperature. By employing this approach, a small library of amine-linked 2,4,6-trisubstituted pyrimidines with 99 candidates was successfully constructed for SAR study. Similarly, pyrimidines **14** with a sulfonamide group were also synthesized for SAR study, and their synthesis route is depicted in Scheme 2. Treatment of selected bromides **13ay** and **13az** with excess 1-Boc-homopiperazine afforded Boc-protected pyrimidines **14** (**14ay_amine40** and **14az_amine40**), respectively, in high yield, which were further acidified with trifluoroacetic acid (TFA) in dichloromethane (DCM) to furnish pyrimidines **14** (**14ay_amine41** and **14az_amine41**) with a secondary amino group. Pyrimidines **14** (**14az_amine42−47**) with a sulfonamide group were successfully synthesized in good yield by treating various commercially available sulfonyl chlorides with amine **14az_amine41**.

2.2. Evaluation of Antimicrobial Activities, SAR, and Cytotoxicity against Normal Cells. The compound library of 2,4,6-trisubstituted pyrimidines **14** was then evaluated simultaneously for (1) their antimicrobial activities against the Gram-positive *S. aureus* strain ATCC 29213 and the Gram-negative *E. coli* strain ATCC 25922 by measuring their MIC, which is the lowest concentration of a compound that prevents the visible growth of bacteria in a broth dilution susceptibility test according to the Clinical and Laboratory Standards Institute (CLSI) guidelines,[37] and (2) their cytotoxicity against normal mouse fibroblasts L929 by measuring their IC_{50}, which is the concentration of a compound that is required for 50% inhibition. Parent compounds **7a** and **7b** (Figure 1, bottom right) were selected as a positive control. Their antimicrobial activities against both the bacterial strains ranged from 24 to 64 μg/mL, demonstrating only moderate antibacterial activity and poor selectivity of killing between the two bacterial strains (Table 1, entries 1 and 2). By employing progressive MIC screening together with cytotoxicity assay, we have successfully identified several compounds that displayed superior antimicrobial activity and selectivity against *S. aureus*. The results of

DOI: 10.1021/acsomega.7b00701
ACS Omega 2017, 2, 7281−7292

MIC screening and cytotoxicity assay are summarized in Table 1, in which only compounds with MIC values against *S. aureus* 29213 less than 8 μg/mL are shown. Compounds with MIC values higher than 8 μg/mL are shown in the Supporting Information (Table S1). In general, among all newly synthesized derivatives, most of them displayed potent inhibitory activities against the growth of *S. aureus* along with some extent of cytotoxicity against normal cells L929. The low IC_{50} values of L929 indicate that the compounds are very toxic and may have unselective interaction with protein targets other than FtsZ, causing high cytotoxicity against normal cells. However, all of them exhibited very weak inhibitory activities against the growth of *E. coli* even at a concentration of 64 μg/mL. Such a weak activity against *E. coli* may be attributed to their poor penetration ability into the cytoplasm of Gram-negative bacteria, which have an outer membrane of low permeability. From the compounds listed in Table 1, seven compounds displaying superior potency with MIC values at 3−4 μg/mL were identified, namely, **14dv_amine16**, **14dv_amine06**, **14dv_amine20**, **14dv_amine07**, **14dv_amine08**, **14av_amine16**, and **14av_amine20** (Table 1, entries 3−9). Compared with compound **7b**, their potencies were dramatically improved by 16−21-fold. Interestingly, these compounds possess the common structural features of a 4-pyridyl (4-Py) group at position 2 and a cyclic seven-member homopiperazine ring substituted with a benzyl group at position 4. Detailed SAR analysis of 2,4,6-trisubstituted pyrimidine **14** derivatives is depicted in Figure 2. For the pyrimidine head, the 4-Py group of R^2 of **14av_amine16** was very important for potent antibacterial activity. Replacing this functional group with others such as 3-pyridyl of **14ay_amine16**, 2-pyridyl of **14az_amine16**, phenyl of **14ax_amine16**, and methyl groups of **14aw_amine16** resulted in a weak antibacterial activity, implying that the nitrogen atom of the 4-Py group is crucial for maintaining potent antibacterial activity. For R^1 group of the pyrimidine head, both the phenyl of **14dv_amine16** and the 3-pentyl group of **14av_amine16** were favorable substituents. The less bulky isopropyl group of **14bv_amine16** and the linear *n*-pentyl group of **14cv_amine16** both caused poor antibacterial activity. In general, pyrimidine head bearing 4-Py group of R^2 and phenyl or 3-pentyl groups of R^1 exhibited the most potent antibacterial activity. For SAR analysis of the amine tail (**14av_amine01−14av_amine39**), there were two important structural features that gave rise to potent antibacterial activity: (1) the cyclic seven-member homopiperazine ring with a substituted benzyl group and (2) the benzyl group substituted with a bulky group (*tert*-butyl of **14av_amine07**, trifluoromethyl of **14av_amine16**, isopropyl of **14av_amine06**, and bromo of **14av_amine08**) at the para position, but not at the meta or ortho position, of **14av_amine17−18**. Replacing the amine tail with a cyclic six-member piperazine ring of **14av_amine24**, linear 1,2-diamine of **14av_amine35−36**, or 1,3-diamine of **14av_amine37−38** resulted in a poor antibacterial activity. It is also worthy to note that replacing the benzylic carbon with a rigid functional group, such as carbonyl group of **14av_amine19**, sulfonyl group of **14az_amine43−44**, or α,β-unsaturated ketone group of **14av_amine21−23**, caused a poor antibacterial activity. These results suggested that a more flexible and freely rotatable functional group should be installed at this position. This observation was further supported by the low MIC value of compound **14av_amine20**, in which the benzylic carbon was replaced with a freely rotatable CH_2CH_2 group.

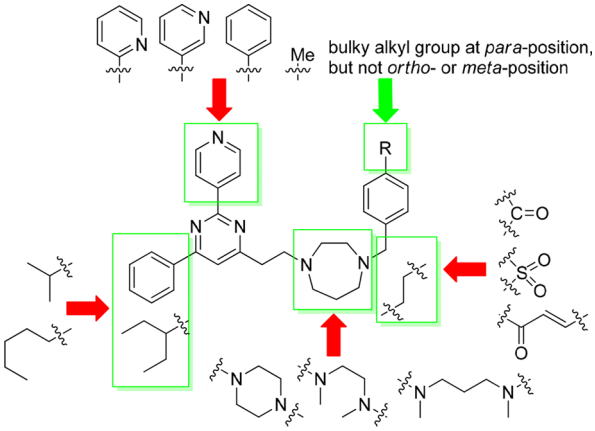

Figure 2. Summary of the SAR study. The red arrows indicate unfavorable substituents. The green arrow and the green boxes indicate favorable substituents.

Encouraged by these promising results, three compounds, namely, **14av_amine16**, **14dv_amine16**, and **14dv_amine06**, were further selected to test against nine clinically isolated bacterial strains including *S. aureus* ATCC 29247, which is an ampicillin-resistant strain, *S. aureus* ATCC BAA-41, ATCC BAA-1717, ATCC BAA-1720, and ATCC 43300 which are methicillin-resistant strains, and four USA300 strains (#417, #757, #1799, and #2690), which are the predominant strain type of community-associated MRSA in the United States. PC190723[38] and compound **5**[29] were also synthesized according the literature for a positive control. The MIC screening results are summarized in Table 2. All compounds were found to retain potent antibacterial activities against these antibiotic-resistant strains with MIC values ranging from 1 to 6

Table 2. MIC Values of Selected Pyrimidines against Nine Clinically Isolated *S. aureus* Strains[a]

	MIC (μg/mL)								
compound no.	strain 1	strain 2	strain 3	strain 4	strain 5	strain 6	strain 7	strain 8	strain 9
PC190723	1	1	1	1	1	1	1	1	1
5	2	2	2	2	4	2	2	2	2
14av_amine16	4	4	6	6	6	6	6	6	6
14dv_amine16	3	3	6	6	6	6	6	6	6
14dv_amine06	3	3	6	6	6	6	6	6	6
methicillin	N.D.	>64	>64	>64	>64	>64	64	64	32

[a]N.D.: not determined; strain 1: ATCC 29247; strain 2: ATCC BAA-1717; strain 3: ATCC BAA-1720; strain 4: ATCC BAA-41; strain 5: ATCC 43300; strain 6: USA300 #417; strain 7: USA300 #757; strain 8: USA300 #1799; and strain 9: USA300 #2690.

DOI: 10.1021/acsomega.7b00701
ACS Omega 2017, 2, 7281−7292

μg/mL. Compounds **14av_amine16**, **14dv_amine16**, and **14dv_amine06** displayed a potent antibacterial activity against MRSA, with MIC values of 3−6 μg/mL, which are very close to those of reported FtsZ inhibitors (**5** and PC190723). Compared with methicillin, which is the clinically used antibiotic with MIC values higher than 64 μg/mL against most of the MRSA, these pyrimidine derivatives exhibited significantly lower MIC values and thus exhibited the potential to be developed into new antistaphylococcal agents in the future. It is worthy to mention that compound **7** did not exhibit any antibacterial activity against these clinically isolated *S. aureus* strains (MIC > 48 μg/mL).

2.3. Investigation of the Potential for the Development of Resistance and in Vivo Biological Evaluation. A crucial attribute of potential antimicrobial agents is that the spontaneous development of drug resistance is not easily attained. To evaluate the spontaneous resistance rate of these compounds in MRSA, compound **14av_amine16** was selected for the study against the MRSA strain ATCC 43300. We plated 1×10^9 cells on agar plates containing 1% dimethyl sulfoxide (DMSO) or 8× the MIC of compound **14av_amine16** and observed the degree of bacterial growth. As shown in Figure 3A (left), almost confluent bacterial growth was observed for the DMSO-treated bacterial cells, yet no colony was observed for the plates treated with compound **14av_amine16** (Figure 3A, right) after 48 h incubation, implying that the rate of emergence of spontaneous resistant mutants was as low as $<1 \times 10^9$. This low frequency of spontaneous resistance implies a reduced probability of rapid development of resistance against compound **14av_amine16** in clinical practice.

As a preliminary measure of in vivo toxicity and efficacy, we next tested our lead compound **14av_amine16** in a *Galleria mellonella* model, which is an easy and inexpensive in vivo model with no ethical constraints for investigating the antibacterial activity of a compound.[39] To examine the feasibility of using *G. mellonella* for compound **14av_amine16** toxicity study, we examined the ability of compound **14av_amine16** to kill *G. mellonella* larvae. Various concentrations of compound **14av_amine16** dissolved in 50% poly(ethylene glycol) (PEG) in saline (0, 50, and 100 mg/kg) were injected into the hemocoel of last-instar *G. mellonella* larvae, and survival was scored over time. All concentrations of compound **14av_amine16** tested did not kill the *G. mellonella* larvae during a 48 h period (Figure 3B). These data indicate that the formulation of 50% PEG in saline and compound **14av_amine16** are nontoxic and safe against *G. mellonella* larvae. Next, we investigated the efficacy of compound **14av_amine16** against *G. mellonella* larvae infected with MRSA ATCC 43300 (Figure 3C). Inoculation of lethal dose of 2.5×10^6 CFU/larva of MRSA ATCC 43300 led to a significant death rate. All larvae injected with 50% PEG in saline (0 mg/kg) died within a 24 h infection period. Injection of compound **14av_amine16** at a dose of 50 mg/kg to the infected larvae was found to prolong the survival time of the infected larvae to 36 h. Encouragingly, we observed 20% survival rate of the infected larvae over the infection period with increased dosage with this agent at 100 mg/kg. Compared to the vehicle group, it was found to be highly significant ($p < 0.05$). Further increased dosage did not lead to improved efficacy (data not shown). These data indicated that compound **14av_amine16** is capable of preventing or delaying the lethal effect of MRSA ATCC 43300 in *G. mellonella* larvae. This suggests that compound **14av_amine16** has strong potential for animal studies in future.

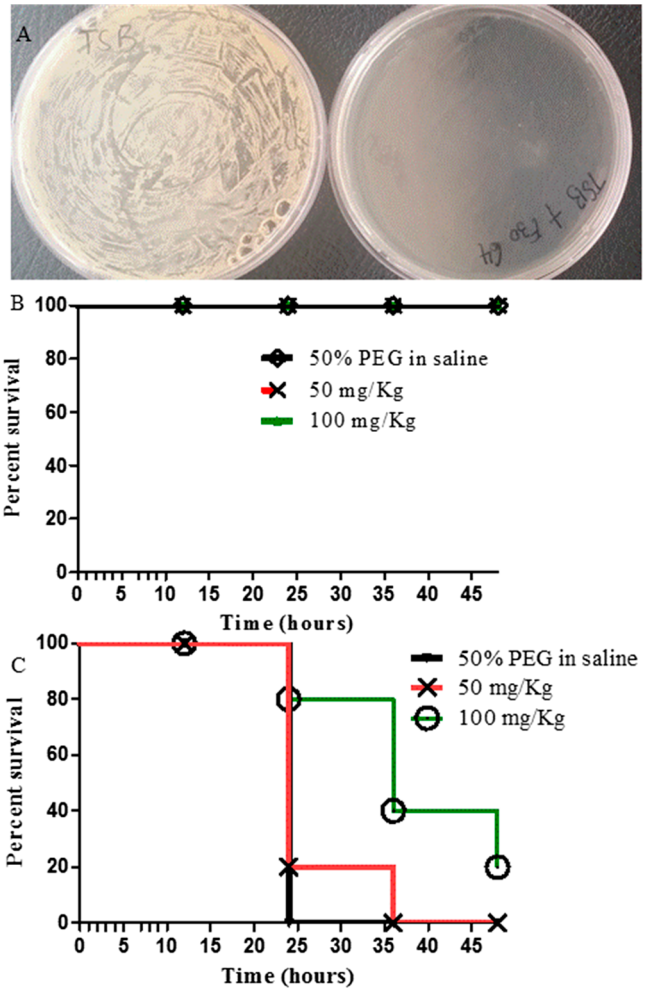

Figure 3. Frequency of resistance (FOR) study (A) and Kaplan−Meier survival analysis of *G. mellonella* larvae following the injection of various concentrations of compound **14av_amine16** without (B) and with (C) lethal dose of MRSA ATCC 43300 inoculation. Larvae were considered dead if they did not respond to physical stimuli. Data presented are the mean of three independent experiments.

2.4. Saturation Transfer Difference NMR Study. Saturation transfer difference (STD) NMR spectroscopy is a powerful and unique tool that can detect the magnetization that was transferred from a protein to a bound ligand proton. It is commonly used to detect the interaction between low-molecular-weight compounds and large biomolecules.[40] To get further insights into the interaction between compound **14av_amine16** and *S. aureus* FtsZ protein, STD NMR spectroscopy was employed to characterize the binding properties and identify the epitopes of small molecules that interact with a protein receptor. *S. aureus* FtsZ protein was expressed and purified as described in a previous report.[29] STD NMR spectroscopy was performed, and the relative degrees of saturation for individual protons of compound **14av_amine16** are displayed in Figure 4, with the integral value of the largest signal set to 100%. The line boarding observed was caused by compound **14av_amine16** being in close contact with the FtsZ protein, resulting in slow tumbling rate of the protein−ligand complex, which also confirmed that compound **14av_amine16** indeed binds to FtsZ protein. All of the protons of compound **14av_amine16** showed some degree of enhancement, demonstrating that the molecule, except the homopiperazine moiety,

DOI: 10.1021/acsomega.7b00701
ACS Omega 2017, 2, 7281−7292

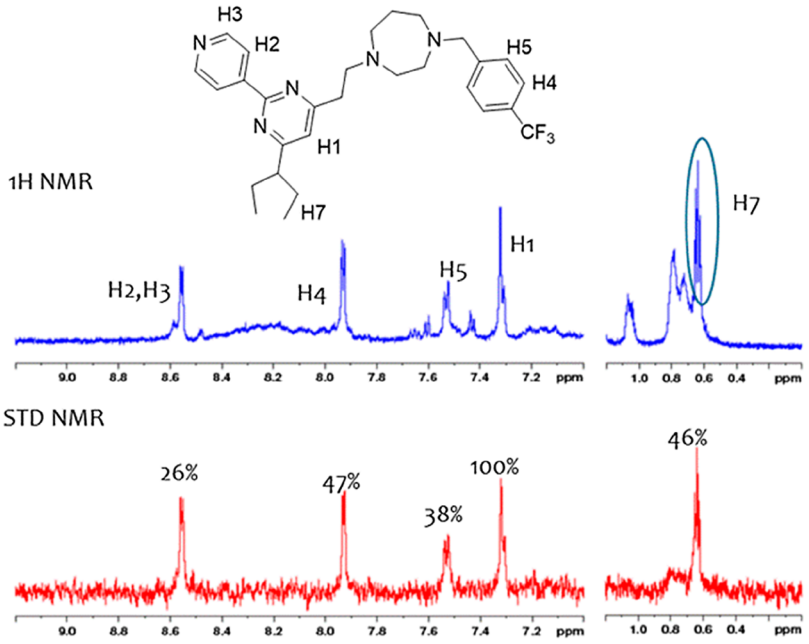

Figure 4. STD effect measured for compound **14av_amine16** binding to *S. aureus* FtsZ protein. Chemical structure and proton assignments of compound **14av_amine16** (upper panel); 1D (STD-off) spectrum displayed in blue with signal assignment (middle panel); and STD spectrum displayed in red (lower panel), and STD effects (I_{STD}/I_0) for each proton are reported.

is bound to the FtsZ protein. The largest amount of saturation transfer was observed for H1, indicating that the pyrimidine ring of compound **14av_amine16** is making more intimate contacts with the FtsZ protein.

2.5. *S. aureus* FtsZ Polymerization and GTPase Hydrolysis Assay. Next, we sought to determine whether the binding of compound **14av_amine16** to *S. aureus* FtsZ protein led to a change in the polymerization activity and GTPase activity of the protein itself. To assay the polymerization activity, an in vitro light scattering assay, in which FtsZ polymerization was detected in solution by a time-dependent increase in light scattering as reflected by an increase in solution absorbance at 600 nm, was employed. Figure 5 shows the relative time-dependent absorbance at 600 nm of *S. aureus* FtsZ

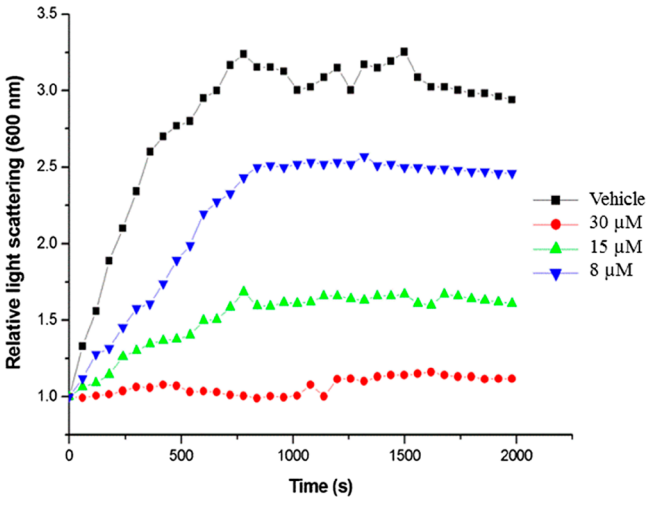

Figure 5. Effect of compound **14av_amine16** at various concentrations on the kinetics of *S. aureus* FtsZ polymerization. The experiments were performed in triplicate, with the symbols indicating the mean value (N = 3).

in the presence of compound **14av_amine16** at concentrations ranging from 0 to 30 μM. It was clearly demonstrated that compound **14av_amine16** potently suppressed the self-polymerization of *S. aureus* FtsZ protein, with the magnitude of these suppressing effects increasing with increasing compound concentration. Compared with the vehicle (1% DMSO), complete inhibition of FtsZ polymerization was observed at 30 μM of compound **14av_amine16**. In addition, we also investigated the inhibitory effect of compound **14av_amine16** on GTPase hydrolysis activity according to the protocol described previously.[33] Compounds **7a** and **7b** inhibited the GTPase hydrolysis activity with IC_{50} values at 73 and 189 μM, respectively. However, compound **14av_amine16** at 50 and 75 μM displayed only moderate inhibition of the GTPase hydrolysis activity at about 20 ± 3% and 25 ± 4%, respectively. GTPase hydrolysis activity at higher compound concentrations (>80 μM) cannot be measured because of the poor compound solubility, which causes precipitation in aqueous medium. Nonetheless, it seems very likely that compound **14av_amine16** suppresses the self-polymerization of the FtsZ protein, probably via disrupting the GTPase hydrolysis activity of the FtsZ protein.

2.6. Effects on the *Bacillus subtilis* 168 Cell Morphology and Localization of the Z-Ring. The underlying mode of action of the antibacterial activity of compound **14av_amine16** was further investigated by the microscopic observation of a rod-shaped *B. subtilis* 168 cell morphology. Compound **14av_amine16** exhibited antibacterial activity against *B. subtilis* 168 with an MIC value at 12 μM. Treatment of *B. subtilis* cells at a sublethal concentration of compound **14av_amine16** significantly increased the cell length with average cell length > 20 μm (Figure 6B) as compared with the DMSO-treated cells (cell length < 5 μm, Figure 6A). Interestingly, such a phenomenon of cell elongation was also observed for other FtsZ inhibitors reported, strongly suggesting that **14av_amine16** interacts with the FtsZ protein in vivo. The iconic filamentous cell phenotype of FtsZ inhibitors was

DOI: 10.1021/acsomega.7b00701
ACS Omega 2017, 2, 7281−7292

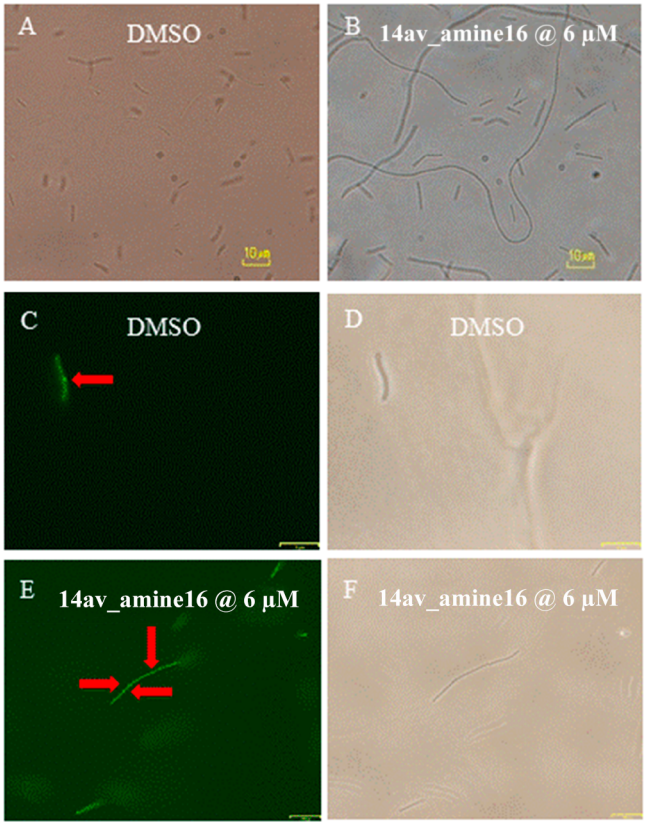

Figure 6. Effects of DMSO or compound **14av_amine16** treated on the cell morphology of *B. subtilis* 168 (A,B), *B. subtilis* 168 with a functional green fluorescent protein-tagged FtsZ (C,E), and their corresponding phase-contrast microscopic pictures (D,F).

believed to be caused by the disruption and mislocalization of the Z-ring. To further confirm that, a fluorescence microscopic analysis of dynamic Z-ring formation in *B. subtilis* 168 was carried out by using a functional green fluorescent protein-tagged FtsZ in *B. subtilis* 168. In the absence of compound (DMSO-treated), fluorescent foci corresponding to the Z-ring formation were observed at the mid cell. Each cell possesses only one fluorescent focus, indicating the proper Z-ring formation and localization (Figure 6C, red arrow). By contrast, upon exposure to compound **14av_amine16**, the bacteria cell lacked mid-cell foci. Instead, the FtsZ protein was randomly distributed as multiple discrete foci (Figure 6E, red arrows) throughout the whole elongated cell, demonstrating that compound **14av_amine16** caused obvious mislocalization of the Z-ring.

3. CONCLUSIONS

In this study, a total of 99 amine-linked 2,4,6-trisubstituted pyrimidines, many displaying potent antistaphylococcal activity and some extent of cytotoxicity against normal cells, has been synthesized systematically by varying the substitutions in 2, 4, and 6 positions. These compounds also exhibited potent antibacterial activities against clinically isolated MRSA strains. These promising results led to the efficacy testing of the lead compound **14av_amine16**, which revealed a very low spontaneous FOR and limited toxicity against *G. mellonella* larvae. Investigation of the mode of action suggests that compound **14av_amine16** exerted its antibacterial activity by interacting with *S. aureus* FtsZ protein and suppressing its polymerization, resulting in obvious mislocalization of the Z-ring formation. In summary, these newly synthesized 2,4,6-trisubstituted pyrimidine derivatives represent a novel scaffold of FtsZ inhibitors.

4. EXPERIMENTAL SECTION

4.1. Chemical Synthesis. All NMR and mass spectra were recorded on a Bruker Avance-III spectrometer and a Micromass Q-TOF-2 spectrometer by the electrospray ionization (ESI) mode, respectively. STD NMR experiments were performed on a Bruker Avance III 600 NMR spectrometer equipped with a QCI cryoprobe at 298 K. All reagents and solvents were of reagent grade and were used without further purification unless otherwise stated. The thin-layer chromatography (TLC) plates (silica gel $60F_{254}$, 0.25 mm thickness) were purchased from E. Merck. Flash column chromatographic purifications were performed on MN silica gel 60 (230−400 mesh). Compound purity was determined by an Agilent 1100 series high-performance liquid chromatography (HPLC) system installed with a Prep-Sil scalar column (4.6 mm × 250 mm, 5 μm) at an UV detection of 254 nm (reference at 450 nm). All tested compounds were shown to have >95% purity according to HPLC. **Amine20** was prepared from homopiperazine and 1-(2-bromoethyl)-4-trifluoromethylbenzene. **Amine38** was prepared from *N*,*N*-diethyl-1,3-diaminopropane and 4-(trifluoromethyl)-benzyl bromide. Other amines used in this study are commercially available.

4.2. General Procedure I for the Synthesis of Pyrimidines 11. To a well-stirred solution of $Pd(PPh_3)_2Cl_2$ (0.4 mmol) and CuI (0.8 mmol) in degassed THF (150 mL) under a nitrogen atmosphere, were added NEt_3 (13 mmol), acid chloride **8** (10 mmol), and alkyne **9** (10 mmol) successively. The reaction mixture was stirred for 3 h until complete conversion as monitored by TLC. After that, Na_2CO_3 (34 mmol) and amidinium hydrochloride salt **10** (12 mmol) were added to the reaction mixture. The resulting suspension was heated to reflux for 14 h. After cooling to room temperature, the reaction mixture was filtered through a short pad of silica gel to remove excess Na_2CO_3. The obtained pale brown filtrate was evaporated under reduced pressure to crude oil which was further subjected to flash column chromatography on silica gel with gradient elution (5% ethyl acetate (EA) in Hex to 30% EA in Hex) to furnish the desired product **11**.

*4.2.1. 4-(2-((tert-Butyldimethylsilyl)oxy)ethyl)-6-(pentan-3-yl)-2-(pyridin-4-yl)pyrimidine (**11av**).* The titled compound **11av** was obtained as a colorless oil (0.32 g, 83% yield) according to the general procedure I described above: ^{1}H NMR (400 MHz, $CDCl_3$): δ 8.76 (d, J = 4.40 Hz, 2H), 8.35 (d, J = 5.87 Hz, 2H), 7.03 (s, 1H), 4.10 (t, J = 6.11 Hz, 2H), 3.01 (t, J = 6.11 Hz, 2H), 2.50−2.64 (m, 1H), 1.69−1.87 (m, 4H), 0.77−0.88 (m, 15H), −0.02 (s, 6H); ^{13}C NMR (101 MHz, chloroform-*d*): δ 173.8, 168.2, 161.9, 150.3, 145.7, 122.2, 119.9, 61.9, 51.0, 41.2, 27.5, 25.8, 18.2, 12.0, −5.5; LRMS (ESI) m/z: 386 (M^+ + H, 100); HRMS (ESI) calcd for $C_{22}H_{36}N_3OSi$ (M^+ + H), 386.2628; found, 386.2621.

4.3. General Procedure II for the Synthesis of Alcohols 12. To a well-stirred solution of pyrimidine **11** (5 mmol) in methanol (20 mL) at room temperature, was added excess concn hydrochloric acid (5 mL) dropwise. The reaction mixture was stirred for 2 h until complete conversion as monitored by TLC. After that, 2 M NaOH solution was added to neutralize the reaction mixture (pH 7), followed by extraction with DCM. The combined organic layers were

DOI: 10.1021/acsomega.7b00701
ACS Omega 2017, 2, 7281−7292

dried over $MgSO_4$, filtered, and evaporated to afford the desired product **12**, which is pure enough for the next step.

*4.3.1. 2-(6-(Pentan-3-yl)-2-(pyridin-4-yl)pyrimidin-4-yl)-ethanol (**12av**).* The titled compound **12av** was obtained as a colorless oil (0.27 g, quantitative yield) according to the general procedure II described above: ^{1}H NMR (400 MHz, $CDCl_3$): δ 8.46 (d, J = 4.40 Hz, 2H), 8.15 (d, J = 5.87 Hz, 2H), 6.96 (s, 1H), 5.00 (br, OH, 1H), 4.00 (t, J = 6.11 Hz, 2H), 3.36 (t, J = 6.11 Hz, 2H), 2.56−2.63 (m, 1H), 1.71−1.88 (m, 4H), 0.83 (t, J = 6.11 Hz, 6H); ^{13}C NMR (101 MHz, $CDCl_3$): δ 175.3, 168.5, 161.3, 149.8, 145.8, 122.1, 118.0, 60.1, 40.8, 30.5, 27.9, 12.0; LRMS (ESI) m/z: 272 (M^+ + H, 100); HRMS (ESI) calcd for $C_{16}H_{22}N_3O$ (M^+ + H), 272.1763; found, 272.1750.

4.4. General Procedure III for the Synthesis of Bromides 13. To a well-stirred solution of alcohol **12** (3 mmol) and PPh_3 (3.6 mmol) in THF (50 mL) at room temperature, was added carbon tetrabromide (3.6 mmol) once. The reaction mixture was stirred for 3 h until complete conversion as monitored by TLC. The reaction mixture was filtered through a short pad of silica gel. The obtained pale brown filtrate was evaporated under reduced pressure to crude oil which was further subjected to flash column chromatography on silica gel with gradient elution (5% EA in Hex to 20% EA in Hex) to furnish the desired product **13**.

*4.4.1. 4-(2-Bromoethyl)-6-(pentan-3-yl)-2-(pyridin-4-yl)-pyrimidine (**13av**).* The titled compound **13av** was obtained as a colorless oil (0.27 g, 80% yield) according to the general procedure III described above: ^{1}H NMR (400 MHz, $CDCl_3$): δ 8.77 (dd, J = 1.47, 4.40 Hz, 2H), 8.26−8.42 (m, 2H), 6.99 (s, 1H), 3.88 (t, J = 6.60 Hz, 2H), 3.37 (t, J = 6.85 Hz, 2H), 2.51−2.67 (m, 1H), 1.69−1.89 (m, 4H), 0.84 (t, J = 7.34 Hz, 6H); ^{13}C NMR (101 MHz, $CDCl_3$): δ 174.5, 166.5, 162.2, 150.3, 145.4, 122.2, 119.4, 51.0, 40.4, 30.1, 27.5, 12.0; LRMS (ESI) m/z: 334 (M^+ + H, 100); HRMS (ESI) calcd for $C_{16}H_{21}N_3Br$ (M^+ + H), 334.0919; found, 334.0914.

4.5. General Procedure IV for the Synthesis of Pyrimidines 14. To a well-stirred solution of slightly excess amine (1.1 mmol) in ACN (10 mL) at room temperature, was added a freshly prepared bromide **13** (1 mmol) solution in ACN (10 mL) once. The reaction mixture was stirred for 14 h until complete conversion as monitored by TLC. The reaction mixture was evaporated under reduced pressure to crude oil which was further subjected to flash column chromatography on silica gel with gradient elution (1% MeOH in DCM to 5% MeOH in DCM) to furnish the desired product **14**.

*4.5.1. 1-(2-(6-(Pentan-3-yl)-2-(pyridin-4-yl)pyrimidin-4-yl)-ethyl)-4-(4-(trifluoromethyl)benzyl)-1,4-diazepane (**14av_amine16**).* The titled compound **14av_amine16** was obtained as a colorless oil (0.27 g, 53% yield) according to the general procedure IV described above: ^{1}H NMR (400 MHz, $CDCl_3$): δ 8.72−8.80 (m, 2H), 8.31−8.38 (m, 2H), 7.52−7.60 (m, J = 8.31 Hz, 2H), 7.40−7.49 (m, J = 8.31 Hz, 2H), 6.99 (s, 1H), 3.67 (s, 2H), 2.96−3.08 (m, 4H), 2.83−2.90 (m, 2H), 2.77−2.83 (m, 2H), 2.66−2.72 (m, 4H), 2.57 (tt, J = 5.81, 8.38 Hz, 1H), 1.73−1.87 (m, 6H), 0.83 (t, J = 7.58 Hz, 6H); ^{13}C NMR (101 MHz, $CDCl_3$): δ 173.9, 169.0, 161.9, 150.3, 145.7, 143.9, 128.8, 125.6, 125.2, 125.1, 125.1, 125.1, 122.9, 122.2, 119.1, 62.2, 57.2, 55.3, 55.2, 54.3, 53.9, 51.0, 35.9, 27.8, 27.5, 12.0; LRMS (ESI) m/z: 512 (M^+ + H, 100), 534 (M^+ + Na, 13); HRMS (ESI) calcd for $C_{29}H_{37}N_5F_3$ (M^+ + H), 512.3001; found, 512.2986.

4.6. Antimicrobial Susceptibility Tests. The MIC values of all compounds were determined using the broth microdilution procedure in accordance with the CLSI guidelines[37] and our previous reports.[29,44]

4.7. Cytotoxicity (IC_{50}) Assay toward the L929 Cell Line. Standard MTS assay was performed to determine the cytotoxicity of all compounds toward the L929 cells. Briefly, 10 000 cells were mixed with compounds at different concentrations in a final volume of 100 μL in each well of a 96-well plate, followed by 3 days incubation at 37 °C. DMSO at 1% was used as a solvent control. The half-maximal inhibition of the compounds was determined using a CellTiter 96 AQueous assay (Promega). An aliquot of the freshly prepared MTS/phenazine methosulfate mixture at a ratio of 20:1 was added into each well, followed by 2 h incubation at 37 °C. Optical absorbance at 490 nm was measured with a microplate reader. The IC_{50} values were determined from the dose−response curves of the MTS assay (Prism 4.0). All experiments were performed in triplicates, and the results will be presented as the average of the three independent measurements.

4.8. Expression and Purification of *S. aureus* FtsZ Protein. Expression and purification of *S. aureus* FtsZ protein were performed as previously reported, which was stored at −20 °C as a lyophilized powder.[29,44] A stock solution of the FtsZ protein was then prepared from the lyophilized powder for subsequent STD NMR study, light scattering assay, and GTPase activity assay.

4.9. STD NMR Study. The STD NMR study of compound **14av_amine16** was performed according to our previous report.[42] Group epitope mapping was performed by integrating the STD signal of the individual protons with respect to the strongest STD signal, which was assigned to a value of 100%.

4.10. Light Scattering Assays and GTPase Activity Assays. The light scattering assays and GTPase activity assays were performed as previously described.[29,34,44]

4.11. FOR Determination. MRSA ATCC 43300 cells were grown to the late-exponential phase (1×10^9 CFU/mL) and spread on agar plates containing 1% DMSO or compound **14av_amine16** at 8 folds of MIC level. The plates were incubated for 48 h to allow resistant mutants to grow. The spontaneous FOR was calculated as the number of resistance colonies divided by the number of CFUs originally plated. The assay was performed in triplicates.

4.12. Evaluation of Toxicity and Antimicrobial Efficacy Using a *G. mellonella* Model of Infection. A *G. mellonella* model of *S. aureus* infection was adopted to test the in vivo toxicity and efficacy of compound **14av_amine16** according to previous reports.[41,43] Groups of *G. mellonella* larvae (N = 10) weighing 200−300 mg were used in these assays. All larvae were incubated at 37 °C, and the mortality rates were assessed at 12 h interval for 48 h after different treatments. All larvae were scored as dead if they showed no signs of movement to physical stimuli. All injections were carried out into the last left proleg of the larvae using a 10 μL Hamilton syringe. For toxicity evaluation, the larvae were injected with 0 (vehicle), 50, and 100 mg/kg compound **14av_amine16** only. For antimicrobial efficacy, the larvae were inoculated with a lethal dose of 10 μL of *S. aureus* 43300 (2.5×10^6 CFU). All larvae received compound **14av_amine16** of different dosages (0, 50, and 100 mg/kg) 1 h before bacterial inoculation. All data were analyzed for statistical significance using a log rank and χ squared test with 1° of freedom.

DOI: 10.1021/acsomega.7b00701
ACS Omega 2017, 2, 7281−7292

4.13. Bacterial Morphology of *B. subtilis* 168. The bacterial morphology study of *B. subtilis* 168 was performed under a phase-contrast optical microscope as previously described.[29,44]

4.14. Z-Ring Visualization of *B. subtilis* 168. The study of Z-ring visualization of *B. subtilis* 168 was performed under a fluorescence and phase-contrast microscope using the Olympus FSX100 bio imaging navigator software as previously described.[29,44]

■ ASSOCIATED CONTENT

Supporting Information

The Supporting Information is available free of charge on the ACS Publications website at DOI: 10.1021/acsomega.7b00701.

^{1}H NMR, ^{13}C NMR, and mass spectrometry data of all compounds **11**−**14** and ^{1}H and ^{13}C NMR spectra and MIC values of compounds **14** (PDF)

■ AUTHOR INFORMATION

Corresponding Authors

*E-mail: kf.chan@polyu.edu.hk. Phone: +852 34008684. Fax: +852 23649932 (K.-F.C.).

*E-mail: kwok-yin.wong@polyu.edu.hk. Phone: +852 34008686. Fax: +852 23649932 (K.-Y.W.).

ORCID

Kwok-Yin Wong: 0000-0003-4984-7109

Author Contributions

K.-F.C. and N.S. contributed equally. The manuscript was written through the contributions of all authors. All authors have given approval to the final version of the manuscript.

Notes

The authors declare no competing financial interest.

■ ACKNOWLEDGMENTS

We acknowledge the support by the Research Grants Council of Hong Kong (grant no. 15100115), the Innovation and Technology Commission Hong Kong SAR, and The Hong Kong Polytechnic University.

■ ABBREVIATIONS

MRSA, methicillin-resistant *Staphylococcus aureus*; FtsZ, filamenting temperature-sensitive mutant Z; GTPase, guanosine triphosphatase; GTP, guanosine triphosphate; MIC, minimum inhibitory concentration; VREF, vancomycin-resistant *Enterococcus faecium*; SAR, structure−activity relationship; ACN, acetonitrile; TFA, trifluoroacetic acid; DCM, dichloromethane; STD, saturation transfer difference; CLSI, Clinical and Laboratory Standards Institute; CA-MHB, cation-adjusted Mueller Hinton broth; DMSO, dimethyl sulfoxide; TLC, thin-layer chromatography; 4-Py, 4-pyridyl

■ REFERENCES

(1) Klevens, R. M.; Morrison, M. A.; Nadle, J.; et al. Invasive methicillin-resistant staphylococcus aureus infections in the united states. *JAMA, J. Am. Med. Assoc.* **2007**, *298*, 1763−1771.

(2) http://www.cdc.gov/drugresistance/pdf/ar-threats-2013-508.pdf (accessed July 15, 2017).

(3) Lock, R. L.; Harry, E. J. Cell-division inhibitors: new insights for future antibiotics. *Nat. Rev. Drug Discovery* **2008**, *7*, 324−338.

(4) Sass, P.; Brötz-Oesterhelt, H. Bacterial cell division as a target for new antibiotics. *Curr. Opin. Microbiol.* **2013**, *16*, 522−530.

(5) Foss, M. H.; Eun, Y.-J.; Weibel, D. B. Chemical−Biological Studies of Subcellular Organization in Bacteria. *Biochemistry* **2011**, *50*, 7719−7734.

(6) Schaffner-Barbero, C.; Martín-Fontecha, M.; Chacón, P.; Andreu, J. M. Targeting the Assembly of Bacterial Cell Division Protein FtsZ with Small Molecules. *ACS Chem. Biol.* **2012**, *7*, 269−277.

(7) Ma, S.; Ma, S. The Development of FtsZ Inhibitors as Potential Antibacterial Agents. *ChemMedChem* **2012**, *7*, 1161−1172.

(8) Ojima, I.; Kumar, K.; Awasthi, D.; Vineberg, J. G. Drug discovery targeting cell division proteins, microtubules and FtsZ. *Bioorg. Med. Chem.* **2014**, *22*, 5060−5077.

(9) Hurley, K. A.; Santos, T. M. A.; Nepomuceno, G. M.; Huynh, V.; Shaw, J. T.; Weibel, D. B. Targeting the bacterial division protein FtsZ. *J. Med. Chem.* **2016**, *59*, 6975−6998.

(10) Anderson, D. E.; Kim, M. B.; Moore, J. T.; O'Brien, T. E.; Sorto, N. A.; Grove, C. I.; Lackner, L. L.; Ames, J. B.; Shaw, J. T. Comparison of Small Molecule Inhibitors of the Bacterial Cell Division Protein FtsZ and Identification of a Reliable Cross-Species Inhibitor. *ACS Chem. Biol.* **2012**, *7*, 1918−1928.

(11) Li, Y.; Hsin, J.; Zhao, L.; Cheng, Y.; Shang, W.; Huang, K. C.; Wang, H.-W.; Ye, S. FtsZ Protofilaments Use a Hinge-Opening Mechanism for Constrictive Force Generation. *Science* **2013**, *341*, 392−395.

(12) Matsui, T.; Han, X.; Yu, J.; Yao, M.; Tanaka, I. Structural Change in FtsZ Induced by Intermolecular Interactions between Bound GTP and the T7 Loop. *J. Biol. Chem.* **2014**, *289*, 3501−3509.

(13) Haydon, D. J.; Stokes, N. R.; Ure, R.; Galbraith, G.; Bennett, J. M.; Brown, D. R.; Baker, P. J.; Barynin, V. V.; Rice, D. W.; Sedelnikova, S. E.; Heal, J. R.; Sheridan, J. M.; Aiwale, S. T.; Chauhan, P. K.; Srivastava, A.; Taneja, A.; Collins, I.; Errington, J.; Czaplewski, L. G. An inhibitor of FtsZ with potent and selective anti-staphylococcal activity. *Science* **2008**, *321*, 1673−1675.

(14) Haydon, D. J.; Bennett, J. M.; Brown, D.; Collins, I.; Galbraith, G.; Lancett, P.; Macdonald, R.; Stokes, N. R.; Chauhan, P. K.; Sutariya, J. K.; Nayal, N.; Srivastava, A.; Beanland, J.; Hall, R.; Henstock, V.; Noula, C.; Rockley, C.; Czaplewski, L. Creating an Antibacterial with in Vivo Efficacy: Synthesis and Characterization of Potent Inhibitors of the Bacterial Cell Division Protein FtsZ with Improved Pharmaceutical Properties. *J. Med. Chem.* **2010**, *53*, 3927−3936.

(15) Qiang, S.; Wang, C.; Venter, H.; Li, X.; Wang, Y.; Guo, L.; Ma, R.; Ma, S. Synthesis and Biological Evaluation of Novel FtsZ-targeted 3-arylalkoxy-2,6-difluorobenzamides as Potential Antimicrobial Agents. *Chem. Biol. Drug Des.* **2016**, *87*, 257−264.

(16) Kaul, M.; Mark, L.; Zhang, Y.; Parhi, A. K.; LaVoie, E. J.; Pilch, D. S. An FtsZ-Targeting Prodrug with Oral Antistaphylococcal Efficacy In Vivo. *Antimicrob. Agents Chemother.* **2013**, *57*, 5860−5869.

(17) Kaul, M.; Mark, L.; Zhang, Y.; Parhi, A. K.; LaVoie, E. J.; Pilch, D. S. Pharmacokinetics and in vivo antistaphylococcal efficacy of TXY541, a 1-methylpiperidine-4-carboxamide prodrug of PC190723. *Biochem. Pharmacol.* **2013**, *86*, 1699−1707.

(18) Kaul, M.; Mark, L.; Zhang, Y.; Parhi, A. K.; Lyu, Y. L.; Pawlak, J.; Saravolatz, S.; Saravolatz, L. D.; Weinstein, M. P.; LaVoie, E. J.; Pilch, D. S. TXA709, an FtsZ-Targeting Benzamide Prodrug with Improved Pharmacokinetics and Enhanced In Vivo Efficacy against Methicillin-Resistant Staphylococcus aureus. *Antimicrob. Agents Chemother.* **2015**, *59*, 4845−4855.

(19) Lepak, A. J.; Parhi, A.; Madison, M.; Marchillo, K.; VanHecker, J.; Andes, D. R. In Vivo Pharmacodynamic Evaluation of an FtsZ Inhibitor, TXA-709, and Its Active Metabolite, TXA-707, in a Murine Neutropenic Thigh Infection Model. *Antimicrob. Agents Chemother.* **2015**, *59*, 6568−6574.

(20) Stokes, N. R.; Baker, N.; Bennett, J. M.; Berry, J.; Collins, I.; Czaplewski, L. G.; Logan, A.; Macdonald, R.; MacLeod, L.; Peasley, H.; Mitchell, J. P.; Nayal, N.; Yadav, A.; Srivastava, A.; Haydon, D. J. An Improved Small-Molecule Inhibitor of FtsZ with Superior In Vitro Potency, Drug-Like Properties, and In Vivo Efficacy. *Antimicrob. Agents Chemother.* **2013**, *57*, 317−325.

(21) Matsui, T.; Yamane, J.; Mogi, N.; Yamaguchi, H.; Takemoto, H.; Yao, M.; Tanaka, I. Structural reorganization of the bacterial cell-

DOI: 10.1021/acsomega.7b00701
ACS Omega 2017, 2, 7281−7292

division protein FtsZ from Staphylococcus aureus. *Acta Crystallogr., Sect. D: Biol. Crystallogr.* **2012**, *68*, 1175−1188.
(22) Tan, C. M.; Therien, A. G.; Lu, J.; Lee, S. H.; Caron, A.; Gill, C. J.; Lebeau-Jacob, C.; Benton-Perdomo, L.; Monteiro, J. M.; Pereira, P. M.; Elsen, N. L.; Wu, J.; Deschamps, K.; Petcu, M.; Wong, S.; Daigneault, E.; Kramer, S.; Liang, L.; Maxwell, E.; Claveau, D.; Vaillancourt, J.; Skorey, K.; Tam, J.; Wang, H.; Meredith, T. C.; Sillaots, S.; Wang-Jarantow, L.; Ramtohul, Y.; Langlois, E.; Landry, F.; Reid, J. C.; Parthasarathy, G.; Sharma, S.; Baryshnikova, A.; Lumb, K. J.; Pinho, M. G.; Soisson, S. M.; Roemer, T. Restoring Methicillin-Resistant Staphylococcus aureus Susceptibility to β-Lactam Antibiotics. *Sci. Transl. Med.* **2012**, *4*, 126ra35.
(23) Kaul, M.; Parhi, A. K.; Zhang, Y.; LaVoie, E. J.; Tuske, S.; Arnold, E.; Kerrigan, J. E.; Pilch, D. S. A Bactericidal Guanidinomethyl Biaryl That Alters the Dynamics of Bacterial FtsZ Polymerization. *J. Med. Chem.* **2012**, *55*, 10160−10176.
(24) Margalit, D. N.; Romberg, L.; Mets, R. B.; Hebert, A. M.; Mitchison, T. J.; Kirschner, M. W.; RayChaudhuri, D. Targeting cell division: Small-molecule inhibitors of FtsZ GTPase perturb cytokinetic ring assembly and induce bacterial lethality. *Proc. Natl. Acad. Sci. U.S.A.* **2004**, *101*, 11821−11826.
(25) Nepomuceno, G. M.; Chan, K. M.; Huynh, V.; Martin, K. S.; Moore, J. T.; O'Brien, T. E.; Pollo, L. A. E.; Sarabia, F. J.; Tadeus, C.; Yao, Z.; Anderson, D. E.; Ames, J. B.; Shaw, J. T. Synthesis and Evaluation of Quinazolines as Inhibitors of the Bacterial Cell Division Protein FtsZ. *ACS Med. Chem. Lett.* **2015**, *6*, 308−312.
(26) Plaza, A.; Keffer, J. L.; Bifulco, G.; Lloyd, J. R.; Bewley, C. A. Chrysophaentins A−H, Antibacterial Bisdiarylbutene Macrocycles That Inhibit the Bacterial Cell Division Protein FtsZ. *J. Am. Chem. Soc.* **2010**, *132*, 9069−9077.
(27) Marcelo, F.; Huecas, S.; Ruiz-Ávila, L. B.; Cañada, F. J.; Perona, A.; Poveda, A.; Martín-Santamaría, S.; Morreale, A.; Jiménez-Barbero, J.; Andreu, J. M. Interactions of Bacterial Cell Division Protein FtsZ with C8-Substituted Guanine Nucleotide Inhibitors. A Combined NMR, Biochemical and Molecular Modeling Perspective. *J. Am. Chem. Soc.* **2013**, *135*, 16418−16428.
(28) Huecas, S.; Marcelo, F.; Perona, A.; Ruiz-Ávila, L. B.; Morreale, A.; Cañada, F. J.; Jiménez-Barbero, J.; Andreu, J. M. Beyond a Fluorescent Probe: Inhibition of Cell Division Protein FtsZ by mant-GTP Elucidated by NMR and Biochemical Approaches. *ACS Chem. Biol.* **2015**, *10*, 2382−2392.
(29) Sun, N.; Chan, F.-Y.; Lu, Y.-J.; Neves, M. A. C.; Lui, H.-K.; Wang, Y.; Chow, K.-Y.; Chan, K.-F.; Yan, S.-C.; Leung, Y.-C.; Abagyan, R.; Chan, T.-H.; Wong, K.-Y. Rational Design of Berberine-Based FtsZ Inhibitors with Broad-Spectrum Antibacterial Activity. *PLoS One* **2014**, *9*, No. e97514.
(30) Domadia, P. N.; Bhunia, A.; Sivaraman, J.; Swarup, S.; Dasgupta, D. Berberine targets assembly of Escherichia coli cell division protein FtsZ. *Biochemistry* **2008**, *47*, 3225−3234.
(31) Artola, M.; Ruiz-Avila, L. B.; Vergoñós, A.; Huecas, S.; Araujo-Bazán, L.; Martín-Fontecha, M.; Vázquez-Villa, H.; Turrado, C.; Ramírez-Aportela, E.; Hoegl, A.; Nodwell, M.; Barasoain, I.; Chacón, P.; Sieber, S. A.; Andreu, J. M.; López-Rodríguez, M. L. Effective GTP-Replacing FtsZ Inhibitors and Antibacterial Mechanism of Action. *ACS Chem. Biol.* **2015**, *10*, 834−843.
(32) Ruiz-Avila, L. B.; Huecas, S.; Artola, M.; Vergoñós, A.; Ramírez-Aportela, E.; Cercenado, E.; Barasoain, I.; Vázquez-Villa, H.; Martín-Fontecha, M.; Chacón, P.; López-Rodríguez, M. L.; Andreu, J. M. Synthetic Inhibitors of Bacterial Cell Division Targeting the GTP-Binding Site of FtsZ. *ACS Chem. Biol.* **2013**, *8*, 2072−2083.
(33) Chan, F.-Y.; Sun, N.; Neves, M. A. C.; Lam, P. C.-H.; Chung, W.-H.; Wong, L.-K.; Chow, H.-Y.; Ma, D.-L.; Chan, P.-H.; Leung, Y.-C.; Chan, T.-H.; Abagyan, R.; Wong, K.-Y. Identification of a New Class of FtsZ Inhibitors by Structure-Based Design and in Vitro Screening. *J. Chem. Inf. Model.* **2013**, *53*, 2131−2140.
(34) Chan, F.-Y.; Sun, N.; Leung, Y.-C.; Wong, K.-Y. Antimicrobial activity of a quinuclidine-based FtsZ inhibitor and its synergistic potential with β-lactam antibiotics. *J. Antibiot.* **2015**, *68*, 253−258.
(35) O'Shea, R.; Moser, H. E. Physicochemical Properties of Antibacterial Compounds: Implications for Drug Discovery. *J. Med. Chem.* **2008**, *51*, 2871−2878.
(36) Karpov, A. S.; Müller, T. J. J. Straightforward novel one-pot enaminone and pyrimidine syntheses by coupling-addition-cyclo-condensation sequences. *Synthesis* **2003**, 2815−2826.
(37) Clinical and Laboratory Standards Institute. *Methods for Dilution Antimicrobial Susceptibility Tests for Bacteria That Grow Aerobically; Approved Standard*, 7th ed.; CLSI document M07-A7; Clinical and Laboratory Standards Institute: Wayne, PA, 2006.
(38) Sorto, N. A.; Olmstead, M. M.; Shaw, J. T. Practical Synthesis of PC190723, an Inhibitor of the Bacterial Cell Division Protein FtsZ. *J. Org. Chem.* **2010**, *75*, 7946−7949.
(39) Tsai, C. J.-Y.; Loh, J. M. S.; Proft, T. Galleria mellonella infection models for the study of bacterial diseases and for antimicrobial drug testing. *Virulence* **2016**, *7*, 214−229.
(40) Mayer, M.; Meyer, B. Characterization of Ligand Binding by Saturation Transfer Difference NMR Spectroscopy. *Angew. Chem., Int. Ed.* **1999**, *38*, 1784−1788.
(41) Lam, T.; Hilgers, M. T.; Cunningham, M. L.; Kwan, B. P.; Nelson, K. J.; Brown-Driver, V.; Ong, V.; Trzoss, M.; Hough, G.; Shaw, K. J.; Finn, J. Structure-Based Design of New Dihydrofolate Reductase Antibacterial Agents: 7-(Benzimidazol-1-yl)-2,4-diamino-quinazolines. *J. Med. Chem.* **2014**, *57*, 651−668.
(42) Wang, Y.; Chan, F.-Y.; Sun, N.; Lui, H.-K.; So, P.-K.; Yan, S.-C.; Chan, K.-F.; Chiou, J.; Chen, S.; Abagyan, R.; Leung, Y.-C.; Wong, K.-Y. Structure-based design, synthesis, and biological evaluation of isatin derivatives as potential glycosyltransferase inhibitors. *Chem. Biol. Drug Des.* **2014**, *84*, 685−696.
(43) Horn, K. S. V.; Burda, W. N.; Fleeman, R.; Shaw, L. N.; Manetsch, R. Antibacterial Activity of a Series of N2,N4-Disubstituted Quinazoline-2,4-diamines. *J. Med. Chem.* **2014**, *57*, 3075−3093.
(44) Lui, H. K. Alkoxy- and amino-benzamides as inhibitors of the bacterial cell division protein FtsZ and antibacterial agents. M. Phil. Thesis, The Hong Kong Polytechnic University, Hong Kong, 2014.

DOI: 10.1021/acsomega.7b00701
ACS Omega 2017, 2, 7281−7292